REVIEW OF TROPICAL NIGHTGLOW STUDIES WITH ASTRONOMICAL INSTRUMENTS

SUMMARY

Much of upper atmospheric chemistry and physics can be read in the detailed study of the nightglow. There are several classic observables – oxygen green line, oxygen red lines, OH, O_2 Atmospheric 0-1 – but these are chosen for their convenient intensities, not necessarily because they reveal the most about the atmosphere. It has recently become evident that the sky spectra obtained at large telescopes show the nightglow and even glimpses of the dayglow with much more detail than has been previously available. Here we show examples of this new information, attempting to make the case that having such instruments for use by the aeronomic community would have great benefits. A recent review of this work has been published in conjunction with related laboratory experiments.[*Slanger and Copeland*, 2003]

1) Discovery of the O_2(*c*-*b*) Emission Bands

Much of the terrestrial nightglow originates with electronic transitions in O_2. The well-known transitions are the $A^3\Sigma_u^+$ - $X^3\Sigma_g^-$ Herzberg I system, the $b^1\Sigma_g^+$ - $X^3\Sigma_g^-$ Atmospheric system, the $a^1\Delta_g$ - $X^3\Sigma_g^-$ Infrared Atmospheric system, and the $A'^3\Delta_u$ - $a^1\Delta_g$ Chamberlain system, the latter being the only one not terminating on the ground state. The Herzberg II $c^1\Sigma_u^-$ - $X^3\Sigma_g^-$ system, extremely strong in the atmosphere of Venus,[*Krasnopolsky*, 1986] is often included in modeling the spectroscopy of the terrestrial atmosphere, but detailed studies of the Keck data show it to be relatively weak. It would be strongest in the region below 300 nm, inaccessible for ground-based instruments.

Astronomical sky spectra are proving to be a superb tool for carrying out detailed studies of the airglow. Numerous new phenomena have been found in recent years, including the discovery of a new O_2 band system, the $c^1\Sigma_u^-$ - $b^1\Sigma_g^+$ transition.[*Slanger et al.*, 2003b] This is the first identification of an O_2 system with the $b^1\Sigma_g^+$ state as the lower level. The system is easier to identify than the Herzberg II system, and with adequate resolution it is possible to carry out investigations on the $c^1\Sigma_u^-$ state, whose energy transfer to O-atoms has been hypothesized to be the source of the mesospheric oxygen green line.[*Bates*, 1988]

The reason that the *c*-*b* bands have not previously been identified has to do with spectral resolution, and also with the unique spectroscopic signature of the transition. As is the case for all O_2 nightglow systems, the transition is optically forbidden, and must obtain its transition probability by interaction of either the upper or lower level with some other state that confers a finite radiative probability. The $^1\Sigma_u^-$ - $^1\Sigma_g^+$ symmetry of the transition is quite unusual, and the only other known example in a diatomic molecule is an absorption system in N_2.[*Wilkinson and Mulliken*, 1959]

The details are discussed in the published work,[*Slanger et al.*, 2003b] but the consequences are that there is only a Q-branch in the transition with only even rotational levels represented, the density of lines is quite low, the rotational distribution favors high-J levels, and low-v levels do not appear. Because of the low density of lines, it is not possible to monitor a band with coarse resolution – the lines fade into the background. Only with adequate resolution are the lines of the band apparent.

In Figure 1 are shown lines of the *c*-*b* 9-1 band with their identifications from two different sources – the HIRES echelle spectrograph on the Keck I telescope, and the UVES echelle on the VLT telescope. Although the relatively strong Chamberlain 7-5 band runs through this region, one sees that the *c*-*b* lines dominate any other emission. However, because the lines are separated by 0.4-0.6 nm, a 1-nm interference filter will likely capture only one line, which will be indiscernible in the background continuum light. Any observations must be made with an instrument capable of isolating individual lines, which explains why this O_2 system has not previously been identified either in nightglow or laboratory spectra, in spite of the fact that it is now easily discernible. These new observations clearly demonstrate the power of sky spectra as aeronomic tools.

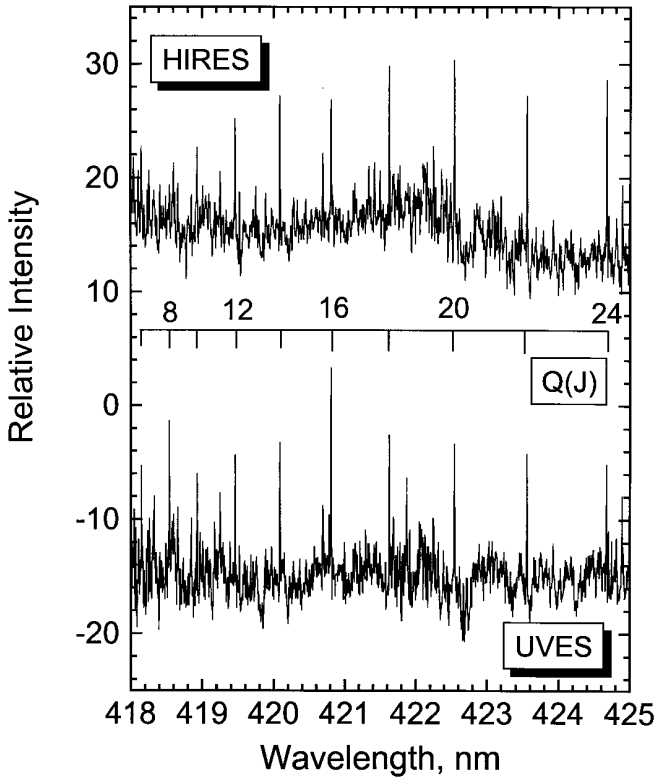

Figure 1. The O_2(*c*-*b*) 9-1 band as seen in co-added spectra from the HIRES and UVES instruments. The alternating Q(J) lines are identified, demonstrating their high intensity at high J. The oscillation in the HIRES baseline is related to the echelle order break at 422 nm. High-J levels of the 10-1 band also appear, cf. the Q(30) line at 420.7 nm.

Interestingly, it is now possible to look at earlier published spectra and see the lines, but no identification was made at the time.[*Chamberlain*, 1958; *Ingham*, 1962] The individual lines of the *c*-*b* bands are as least as bright as the O_2 Herzberg and Chamberlain lines above 400 nm, and even when comparison is made to the stronger Herzberg I bands near the 310 nm ozone cut-off, the *c*-*b* lines still have 25% of the intensity of the lines of the latter.

The *c*-*b* bands can be studied for $c^1\Sigma_u^-$ (v = 4-11), although the v = 9,10 bands are the strongest, their

energies corresponding to the peaks in the population distributions for the other two O_2 Herzberg states, $A^3\Sigma_u^+$ and $A'^3\Delta_u$.[*Slanger et al.*, 2004a] That emission from lower $c^1\Sigma_u^-$ vibrational levels is not seen is not a demonstration that they are not populated. Instead, it reflects that the perturbing state driving the transition lies at energies higher than the $c^1\Sigma_u^-$ state itself, and its effect becomes weaker for the lower $c^1\Sigma_u^-$ vibrational levels.[*Minaev and Yashchuk*, 2004]

2) Ionospheric Emission of the OI Rydberg Series: O^+ Radiative Recombination

The oft-observed 130.4 and 135.6 nm UV oxygen atom emissions, as well as the 844.6 and 777.4 nm IR OI emissions sample the lowest levels of Rydberg series that converge to the ground state of O^+. There are two series – quintets and triplets – with the 844.6 and 130.4 nm lines being the 3p-3s and 3s-2p members of the triplet sequence, and the 777.4 and 135.6 nm lines being the analogs in the quintet series. In both cases the IR emissions immediately precede the UV emissions.

There are different possible sources of these OI levels, particularly in the dayglow, but at night the expectation is that the mechanism is either conjugate photoelectron excitation,[*Lancaster et al.*, 1994; *Lancaster et al.*, 2000] or O^+ radiative recombination[*Tinsley et al.*, 1973]. The radiative recombination process has been previously investigated, but the cross sections are quite small, and even in the tropical nightglow, where charged particle densities can be high, the observed transitions have been limited to the 777.4, 844.6, and 436.8 nm lines, the latter being the 4p-3s triplet transition.

The high sensitivity of the detectors on the Keck telescopes, and the location of the observatory within an Appleton anomaly zone, makes it possible to study the two OI Rydberg series to unexpectedly high levels.[*Slanger et al.*, 2004b] We are able to see the three sequences in each series – ns-3p, np-3s, and nd-3p. In the latter case, the highest level seen is 11d in the quintet sequence, a level lying only 0.11 eV below the O^+ limit.

The fact that these series appear provides strong support for the idea that the process being observed is radiative recombination. Calculations have been carried out on the effective recombination coefficients for the O^+ + e interaction, with all the cascading contributions taken into account.[*Escalante and Victor*, 1992] These calculations are complicated in the case of the triplet series, where multiple resonant scattering becomes a factor. Nevertheless, there is reasonable agreement between the calculated cross sections and the observations, over three orders of magnitude in intensity. This relationship is particularly good for the quintet line sequences, shown in Figure 2. We therefore can conclude that for the conditions at Mauna Kea at the time, the OI Rydberg emissions are generated by radiative recombination.

An additional result of these observations is that it is possible to identify instances when the triplet 844.6 nm emission is seen in the absence of 777.4 and 926.0-926.6 nm quintet emissions, all of which are typically of comparable intensity. The latter is the 3d-3p set of lines.

Such an observation is indicative of a change in production mechanism, and is only observed when the emissions are quite weak. The presence of triplet lines in the absence of quintets suggests an O(^{3}P) photoexcitation mechanism, and indeed, just such a mechanism has been identified from satellite measurements of the O-atom VUV emissions.[*Meier*, 1991] There is a close coincidence between the geocoronal Lyman-beta line at 102.57 nm and the 3d-2p OI Rydberg lines, resulting first in production of an IR photon, and then the 844.6 nm lines. Thus, because of multiple scattering within the hydrogen geocorona this process occurs within the earth's shadow, and in principle the 844.6 nm emission intensity for such conditions could be related to the local O-atom density.

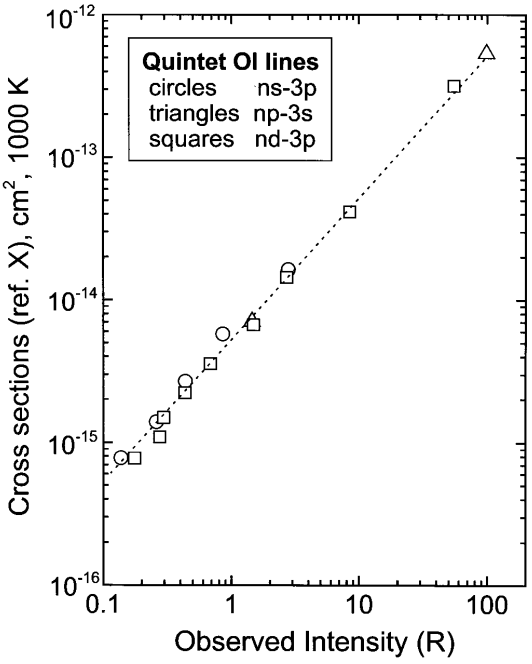

Figure 2. Calculated effective recombination coefficients [*Escalante and Victor*, 1992] *vs* observed Rydberg line intensities in the quintet sequence [*Slanger et al*., 2004]

3) **Variability of the Sodium Nightglow D_2/D_1 Ratio**

Sodium emission at the D_2 and D_1 lines at 589.0 and 589.6 nm is a prominent feature of the terrestrial nightglow and of meteoric trails. Although the spacing between these lines is relatively large, there has been no systematic investigation of their intensity ratio. Instead, the assumption has been made that the ratio should reflect the degeneracies of the J = ½, $^3/_2$ emitters, and therefore must have a value of 2.0. However, the emitting states are produced chemically and will radiate without collisions, while the statistical ratio of 2.0 will result from collisional equilibration at high temperature.

Measurements were carried out at Millstone Hill in 1977 to test the intensity ratio, and in fact a value close to 2.0 was observed, using Fabry-Perot instrumentation.[*Sipler and Biondi*, 1978] It therefore seemed that the nightglow ratio was well-defined. Because we have many hundreds of sky spectra from the two Keck telescopes, and there were indications that the sodium ratio was variable, we undertook an investigation to see if this was indeed the case. It soon became evident that there was great variability in the ratio, and that it was never as large as 2.0.

Subsequently, we learned that sodium ratio measurements had been made at high latitudes in 1975, with the purpose of determining whether the presence of aurora had any effect.[*Rees et al.*, 1975] Most of these measurements were made in the twilight, where solar-excited sodium emission is strong, but observations were continued into the nighttime and it was seen that the ratio was quite variable. However, this was not the emphasis of the study, so the low and apparently noisy nighttime ratios were not pursued. We can now see from the sky spectra studies that these observations were the first indication that the ratio was not fixed.

Figure 3 shows a plot of the hundreds of sodium line ratios that have been measured for 1993-2004, mostly from the Keck I/II telescopes, but also from other sources. Because with these instruments the signal-to-noise ratio is very high, the error bars are quite small, within the symbol size. Therefore the variation is a real effect. The Rees et al. data are incorporated into the plot, as is a series of measurements carried out over the North Atlantic by John Plane [*private communication*, 2003], in the course of a Leonids campaign. A single point is included from the on-line compilation of lines from the UVES/VLT system.

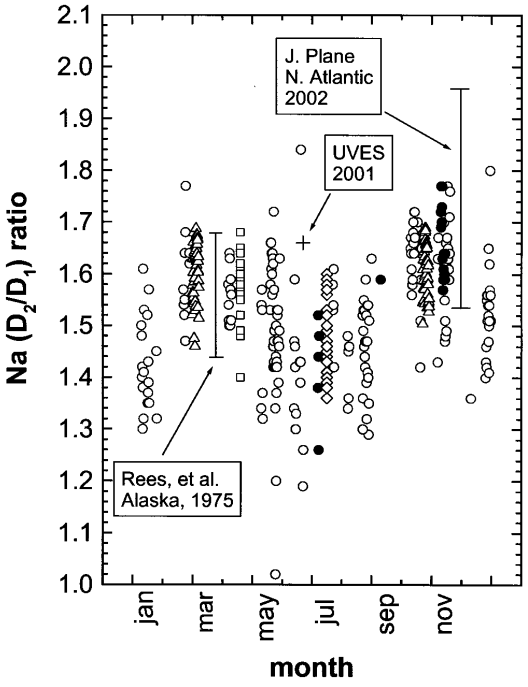

Figure 3. The sodium D_2/D_1 line ratios measured from Keck I/HIRES and Keck II/ESI, 1993-2003. Also shown are the ranges of ratios measured by Rees et al. 1975, and by Plane (private communicatio 2003). A single point from the averaged UVES spectrum is shown.

The data are plotted as a function of month, because the most evident correlation of the ratio values is with season. In fact, a semi-annual oscillation is apparent, with maxima of the ratio at the equinoxes, and minima at the solstices. Such behavior is characteristic of emissions that involve O-atom reactions, such as the green line, the O_2 0-1 Atmospheric band, the Herzberg transitions, and even the sodium lines,[*Kirchhoff and Takahashi*, 1985] where the oscillations are apparent in the emission intensities of these transitions. However, it is not evident why the sodium ratios should behave in a similar manner. Nevertheless, the implication is that the ratios are determined by chemistry, and of course the nightglow emissions are chemically caused, the initial reaction being NaO production from the reaction between a free sodium atom and ozone, and the subsequent reaction being between NaO and an O-atom, which regenerates the Na atom, but in an excited state.

The current thinking is that there are parallel channels for the NaO + O reaction, where both the excited and ground states of NaO are involved. It is possible that there is an additional step in the overall reaction, where the excited NaO is collisionally quenched to ground state NaO by O_2/N_2. If so, it may be that the Na line ratio reflects the [O]/[M] ratio in the emitting region, which would be a very useful metric.

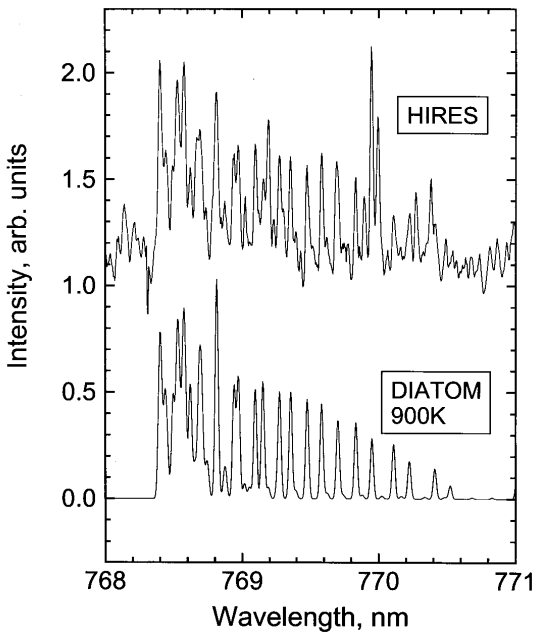

Figure 4. The $O_2(b\text{-}X)$ 1-1 band from ionospheric $O(^1D) + O_2$ energy transfer. The rotational distribution corresponds to a kinetic temperature of about 900K, although in actuality a range of temperatures would be observed [*Slanger et al*., 2003a].

4) The Ionospheric O_2 Nightglow

The molecular oxygen nightglow is usually considered as confined to the region of maximum O-atom density, near 95 km. However, O-atom recombination is not the only way of generating excited O_2 states, and it is possible to find instances of intense O_2 emissions from higher altitudes.

The energy transfer reaction between $O(^1D)$ and O_2 generates the v = 0,1 levels of the $O_2(b^1\Sigma_g^+)$ state with high efficiency.[*Lee and Slanger*, 1978] It should thus be no surprise to find that in the nighttime tropical ionosphere, where the $O(^1D)$ density can be relatively high as a consequence of O_2^+ dissociative recombination, that excited O_2 is formed. As there is relatively intense foreground emission in the *b-X* system, one must find ways to view the ionospheric emission from the ground. The answer lies in taking advantage of the quenching of the foreground emission, revealing the relatively unquenched emission from higher altitudes. Because only two vibrational levels are produced in the $O(^1D) + O_2$ energy transfer, there is a limitation on which bands to study, and it happens that only the *b-X* 1-1 band can be investigated in this way. The unquenched v = 0 emission at 95 km ensures that one cannot see a contribution from higher altitude in either the 0-0 or the 0-1 bands (observation of any but the highest rotational levels in the 0-0 band is in any case precluded by O_2 absorption). From the $b^1\Sigma_g^+$ (v = 1) level, the most intense emission is in the 1-1 band, and the v = 1 levels is strongly quenched by O_2 at 95 km. Thus, one can in principle see the 1-1 band from high altitude, given that it can be distinguished from the lower altitude emission.

Figure 4 shows such an example in a sky spectrum from the HIRES spectrograph. [*Slanger et al.,* 2003a] In fact, the lower altitude emission is relatively unimportant here, and this can be demonstrated by noting that from the rotational distribution it is possible to determine

a temperature for the emitting region. The simulation in Figure 4 shows that the kinetic temperature in the region from which the emission arises is close to 900K, which is well up in the thermosphere. The MSIS-90 model for the date and location gives an exospheric temperature of 890 K and a neutral temperature of 850 K at 200 km.

The emission intensity of the ionospheric *b-X* 1-1 band can be relatively high. From spectra as that shown in Figure 4 , one can make comparisons with the average intensities of OH features, or with the ~1 R potassium D_1 line at 769.9 nm, and 1-1 band values have been obtained in the 100-150 R range. This suggests that from space, and with limb viewing, one can easily obtain both temperatures and altitude distributions of the *b-X* 1-1 band, and of course it is accompanied by the high-altitude 0-0 band which would be at least as intense. In principle the TIDI instrument on the TIMED satellite is capable of observing the tropical ionospheric layer, although the interference filters are not designed to measure high temperatures.

The $b^1\Sigma_g^+$ (v = 0) level will be unquenched in the ionosphere, but the v = 1 level will be strongly quenched, primarily by O-atoms. Because the v = 0 and v = 1 levels are produced with equal yields in the $O(^1D) + O_2$ transfer step, at higher altitudes their emission intensities will be comparable, but with decreasing altitude the v = 1 level will be preferentially quenched, and the [0-0]/[1-1] intensity ratio will increase markedly. This has already been shown in space shuttle spectra from the GLO instrument.[A. L. Broadfoot, private communication] Space-based measurements of the intensity ratio as a function of altitude, at 120-200 km, will directly provide a quenching function. The $b^1\Sigma_g^+$ (v = 1) + O_2 quenching rate coefficient is known,[*Hwang et al.*, 1999] and the rate coefficient for the $b^1\Sigma_g^+$ (v = 1) + $O(^3P)$ interaction has recently been measured in the laboratory.

5) The $O_2(b^1\Sigma_g^+,v)$ distribution

The O_2 Atmospheric band system is generated in the mesosphere by O-atom recombination, and from the ground this system is studied entirely by observation of the *b-X* 0-1 band, at 865 nm. Its typical intensity is 300 R, which makes it an attractive target for observation. However, the high sensitivity of astronomical instruments at large telescopes has made it clear that the 0-1 band is only part of a large array of bands in the O_2 Atmospheric band system, with quite high vibrational levels being reached in the $O_2(b^1\Sigma_g^+)$ state.[*Slanger et al.*, 2000]

Figure 5 shows the nightglow spectrum at 708-720 nm, the region where it was first recognized that there are $b^1\Sigma_g^+$ state vibrational levels above v = 0.[*Osterbrock et al.*, 1996] The identification of the *b-X* 4-3 band confirmed a conjecture[*McDade et al.*, 1986] that excess emission at 714 nm seen in a rocket experiment could be due to this band. Such a result shows the importance of knowing where weak nightglow bands are to be found. We see in Figure 5 that the *b-X* 10-8 band is only a factor of 4-5 weaker than the 4-3 band, and thus the production rates of these higher $b^1\Sigma_g^+$ vibrational levels do not seem to fall off rapidly.

Detailed study of co-added nightglow spectra enabled us to determine the atmospheric distribution. Simultaneously, SRI researchers have evaluated the O_2 and N_2 collisional relaxation rates both for the lower $b^1\Sigma_g^+$ levels, v = 1-3,[*Bloemink et al.*, 1998; *Hwang et al.*, 1999; *Kalogerakis et al.*, 2002] and for high levels, v = 12-15. [*Kalogerakis et al.*, 2001] The former are produced by direct laser excitation of O_2, whereas the latter come from collisional relaxation of laser-excited $O_2(A^3\Sigma_u^+)$ in v = 6-10. In the latter case, there is no $b^1\Sigma_g^+$ state excitation above v = 15, and it is probably not a coincidence that this level is also the highest seen in the atmosphere.

Figure 6 shows the atmospheric $b^1\Sigma_g^+$(v) distribution. Other than the v = 0 population, the highest intensity is associated with the v = 3,4 levels, just those identified in the paper of Osterbrock et al.[1996] There is a second maximum at v = 12, and a deep minimum at v = 8. As collisional removal rates have not been measured for the latter, it is not possible to say whether particularly rapid quenching is responsible.

The distribution is the result of numerous collisional channels that start with the atom recombination process, redistributing the energy to successively lower levels. The vibrational populations are not merely a reflection of collisional loss processes, or at least we do not yet have all the data necessary to make such a claim. Lacking are the O-atom loss rate

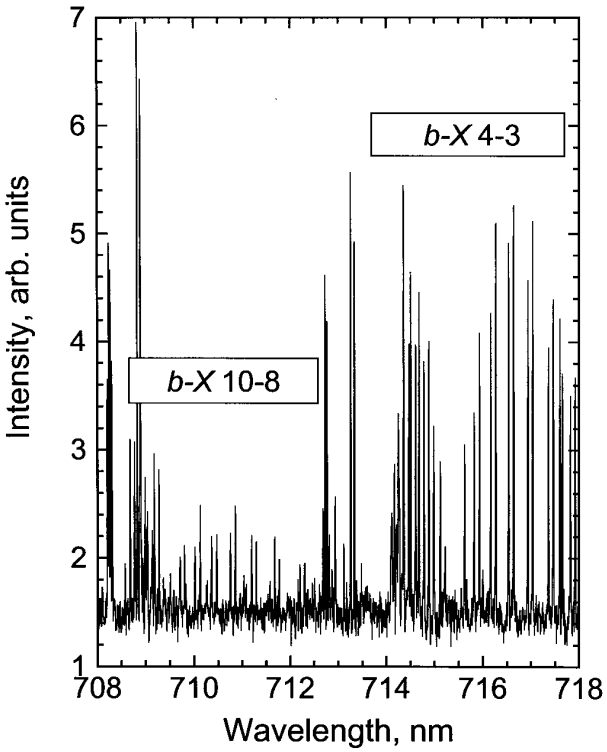

Figure 5. The 708-718 nm region, showing two O_2 Atmospheric bands, UVES

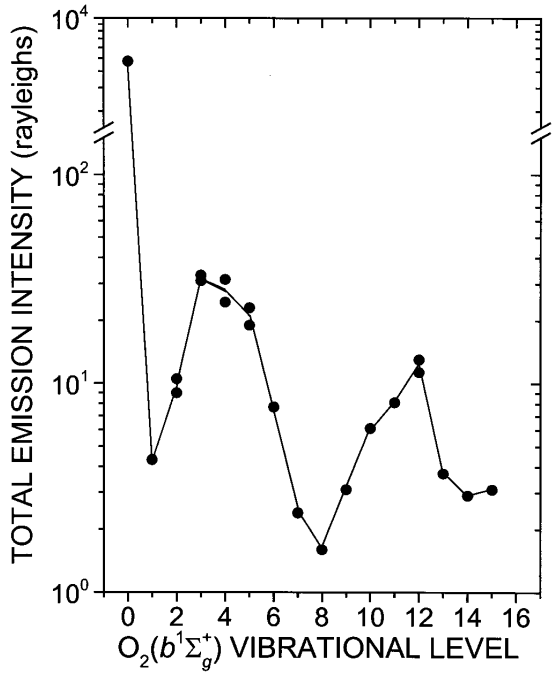

Figure 6. The mesospheric $b^1\Sigma_g^+$(v) distribution [*Slanger et al.*, 2000]

coefficients, which are an important part of any attempt to relate nightglow emission intensities to production rates. Further discussion is found elsewhere.[*Slanger and Copeland*, 2003].

Distributions have now been published for the $O_2(A^3\Sigma_u^+)$ and $O_2(A'^3\Delta_u)$ states in the mesosphere.[*Slanger et al.*, 2004a] Agreement is good with earlier work in the former case, with the addition of significant emission from the v = 0 level. For the $A'^3\Delta_u$ state, the upper state of the Chamberlain bands, the distribution in terms of internal energy is found to mirror the $A^3\Sigma_u^+$ distribution. There is no information on the vibrational distribution of the $a^1\Delta_g$ state, but one can assume that there is little vibrationally-excited population because its radiative lifetime is so long and collisional relaxation of such levels is typically rapid.[*Hwang et al.*, 1998]

6) Chamberlain and Herzberg I band spectroscopy and the $a^1\Delta_g$ and $X^3\Sigma_g^-$ states

High-resolution spectroscopy has been carried out on most O_2 states, because even when the transitions are forbidden, absorption measured at high pressure can still be carried out. However, for the low-lying $a^1\Delta_g$ and $b^1\Sigma_g^+$ states, only the lowest vibrational levels can be accessed in this way. As discussed above, the first data on the high $b^1\Sigma_g^+$ state vibrational levels came from sky spectra.[*Osterbrock et al.*, 1996] In a similar manner, sky spectra provide information on the higher vibrational levels of the $a^1\Delta_g$ state, although not through their emission. Instead, the information comes from Chamberlain band emission, where the $a^1\Delta_g$ state is the lower level.[*Chamberlain*, 1955]

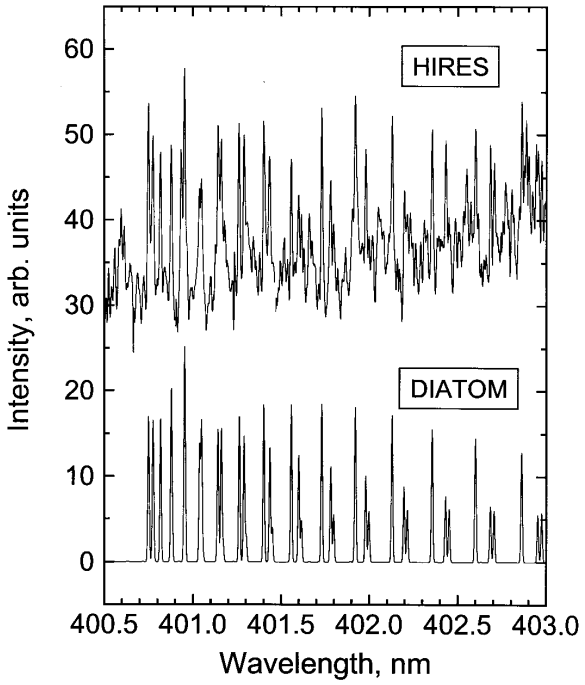

Figure 7. HIRES spectrum of the $O_2(A'^3\Delta_u - a^1\Delta_g)$ 4-3 band, with DIATOM simulation

We have been able to observe many Chamberlain bands in Keck/HIRES and UVES/VLT[*Hanuschik*, 2003] data, with $a^1\Delta_g$ vibrational levels from v = 1 to v = 10. This significantly extends the range for which $a^1\Delta_g$ data exist, and by combining this information with laboratory measurements for $a^1\Delta_g$ (v = 15-19)[*Kalogerakis et al.*, 2000] and electron energy loss spectra up to v = 30,[*Allan*, 1995] it is possible to develop an accurate potential for this state. Figure 7 shows a HIRES spectrum of the Chamberlain 6-2 band.

The $O_2(A^3\Sigma_u^+ - X^3\Sigma_g^-)$ Herzberg I system lies in the same near-UV spectral region, and in a similar manner leads to access of a wide range of vibrational levels in the ground state. We are able to observe emission throughout the $X^3\Sigma_g^-$ (v = 4-15) range, with multiple bands for each ground state level. Existing data on the spectroscopy of vibrationally-excited levels in the ground state comes primarily from O_2 Schumann-Runge band emission, where emission to the higher levels of the ground state is favored. This is not the case for the Herzberg I system, so we are able to get good coverage for the intermediate levels, for which the existing spectroscopic data are significantly poorer than for higher or lower levels. A total of 51 Herzberg I bands can be accurately measured in the sky spectra, and once again we are able to make important advances by using astronomical data. Figure 8 shows a UVES spectrum of the Herzberg I 4-4 band.

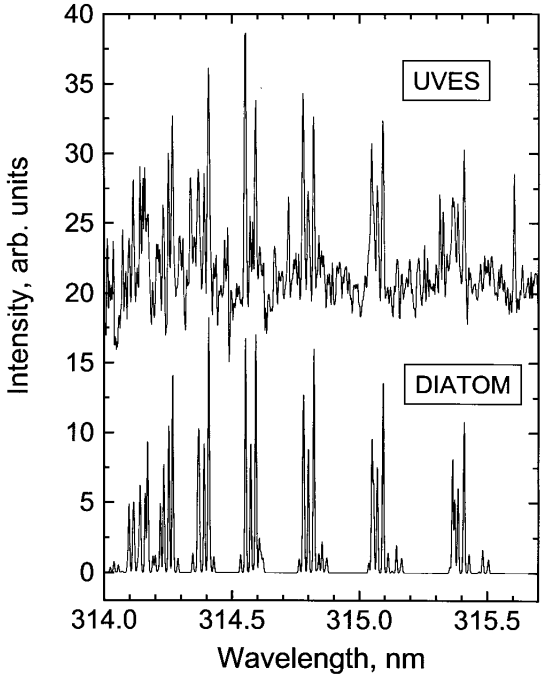

Figure 8. UVES spectrum of the $O_2(A^3\Sigma_u^+ - X^3\Sigma_g^-)$ 4-4 band, with DIATOM simulation

The UVES spectra and line positions are available on line,[*Hanuschik*, 2003] and 2800 lines are tabulated between 314 and 1050 nm. None of these lines are assigned, but this will soon be accomplished, as we have identified thousands of lines in the HIRES spectra. Agreement between the HIRES and UVES line positions is excellent, with an average deviation on the order of 0.0006 nm.

7) Calibrated OH Meinel Band Intensities

The OH radical has been the premier species used to monitor atmospheric changes within the mesosphere [*Sivjee*, 1992]. It is produced primarily by the bimolecular reaction of H atoms with O_3, which is notable in that nearly all of the reaction's substantial exothermicity (3.34 eV) is channeled into high rovibrational excitation of the OH $X^2\Pi$(v,J) product [*Charters, et al.* 1971, *Klenerman and Smith,* 1987]. This nascent excitation, combined with collisional relaxation and radiative cascade, populates a wide range of OH $X^2\Pi$ levels (v = 0-9), which fluoresce as the Meinel bands to create the dominant emission contribution to the earth's nightglow at red and near-infrared wavelengths.

The high efficiency, high resolution, and broad spectral coverage of the echelle spectrographs installed on large astronomical telescopes allow atmospheric Meinel emission to be monitored in exceptional detail as the sky spectrum acquired as a byproduct of celestial observations with long slit instruments.[*Slanger and Osterbrock*, 1998] At visible wavelengths, more than 20 Meinel bands are observed with $\Delta v = v' - v'' = -3$ through -7. Figure 9(a) shows a portion of the night sky spectrum acquired with the ESI spectrograph on the Keck II telescope at Mauna Kea during one 3000 s period on the night of March 4, 2000 at a spectral resolution of $\lambda/\Delta\lambda = 7000$. Even higher resolution sky spectra have been obtained with the HIRES echelle on the Keck I telescope $\lambda/\Delta\lambda = 38{,}000$) and the UVES echelle on the VLT telescope at Cerro Paranal ($\lambda/\Delta\lambda = 50{,}000$).[*Hanuschik,* 2003]

A unique capability of the astronomical spectrographs is that they routinely allow calibration of both the wavelengths and intensities of the spectra. The wavelengths, calibrated during the night using thorium-argon or other standard lamps are consistently accurate to ± 0.0005 nm, allowing confident assignment of the thousands of spectral features that appear in the night sky emission. Intensity calibration is made by observing one or more "standard" stars periodically during the course of the night. Although small uncertainties in the absolute intensity of the nightglow may arise from errors in estimating the fraction of star light collected by the spectrograph, the relative intensity response of the spectrograph as a function of wavelength is precisely defined by comparison to the astronomical photometric standards [*Oke*, 1990, *Colina and Bohlin,* 1994].

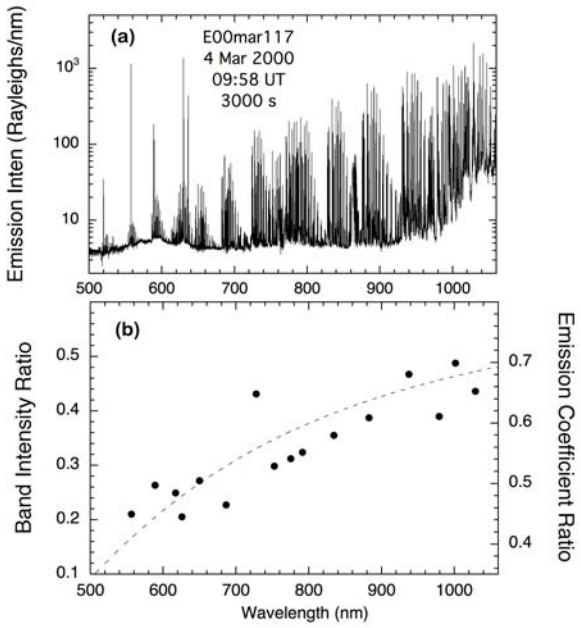

Figure 9. (a). Intensity-calibrated spectrum of night sky emission. (b). Meinel band intensity ratio (points); emission coefficient ratio [*Adler-Golden*, 1997] (dashed line).

Comparison can be made between the Meinel band intensities measured in the calibrated sky spectrum of Figure 9(a) to those previously known from photographic measurements. [*Krassovsky et al.*, 1962] The ratio of the ESI band intensities to those of Krassovsky et al. are shown by the points in Figure 9(b) plotted at the wavelength of the band origin. Although there is considerable scatter in the ratios for individual vibrational bands, possibly due to atmospheric absorption and atomic emission contamination in the relatively low resolution photographic measurements, it is clear that the band intensity ratio systematically changes by approximately a factor of 2 from blue to red wavelengths, consistent with the photographic plates of *Krassovsky et*

al. having an uncorrected lower efficiency in the red. Adler-Golden [1997] had proposed the likelihood of such an error from a comparison of the Meinel band emission coefficients based predominantly on *ab initio* calculations to those that had been adjusted to agree with the Krassovsky et al. intensities. The response curve derived by Adler-Golden, shown by the dashed line in Figure 9(b), closely approximates the observed wavelength dependence of the intensity error.

The Meinel band emission coefficients are essential for converting observed emission intensities into OH column densities, but inconsistencies among the available sets of coefficients has long been noted [*Meriwether*, 1989; *French et al.* 2000] The present availability of the intensity-calibrated Meinel band emission spectra now allows these inconsistencies to be resolved.

8) Investigating Atomic and Chemical Properties of Weak Components of the Nightglow

The high sensitivity and spectral resolution of spectra derived from astronomical instrumentation also accesses nightglow emission from less prevalent atoms and atomic ions. Many of these species express themselves in forbidden transitions which are weak in the quiescent nightglow due to their extremely slow radiative decay time versus collisional de-excitation rate, a factor also precluding laboratory measurements. Other species have extremely low concentrations, necessitating the high sensitivity and resolution of astronomical instrumentation and their spectra to bring out their weak emission from the noise or from behind their stronger OH or O_2 neighbors. Examples of several of the emission lines discussed below, as observed in either Keck/HIRES or VLT/UVES spectra, can be seen in Figure 10.

Because these spectra can be wavelength calibrated to a high degree of accuracy they are ideally suited for measuring transition rest wavelengths. Slanger et al. [2000] compared NIST wavelengths for numerous atomic lines with values measured from a series of 110-200 hour cumulative exposure time co-added Keck/HIRES sky spectra with an estimated accuracy of about 2% of the mean instrumental resolution of 0.02 nm at 750 nm. They found that while well-known, bright nightglow emission lines, such as O(^{1}D-^{3}P) 630.0,636.3 nm, O(^{1}S-^{1}D) 555.7 nm, and Na(D_1,D_2) 589.0,589.6 nm deviated by no more than 0.0004 nm from their NIST values, weaker emission lines such as the forbidden emission of neutral nitrogen, N(^{2}D-^{4}S) 519.8,520.0 nm, and K(D_1) 769.9 nm showed departures two to five times that large. Sharpee et al. [2004] measured the wavelengths of the O^+(^{2}P-^{2}D) doublet components at 732.0 and 733.0 nm from a combination of Keck/HIRES sky spectra and spectra of distant nebulae. The wavelengths of the components of the 732.0 nm doublet were found to differ from the NIST values by 0.012 and 0.013 nm, and the spacing between the doublet components was found to differ by 0.02 nm from the Moore [1949] value of 0.08 nm, which is still used as a figure of merit in estimating the accuracy of fits to Fabry-Perot profiles of these lines.[*Cierpka et al.,* 2003]. The magnitude of the discrepancy between NIST values and those measured in sky spectra are on the order of typical ion-drift velocities of 0.1-0.8 km/s measured by Cierpka et al.[2003]

Some astronomical sky spectra may also be calibrated to absolute intensity units either directly through the use of spectrophotometric standard stars,[*Oke*, 1990] or via knowledge of relative time-averaged OH band intensities.[*Cosby*, 1999] This allows quantitative statements to be made about the efficiency and nature of the mechanisms producing the excited levels giving rise to the emission, as well as the spontaneous emission coefficients that govern the emission. Slanger and Osterbrock [2000] observed potassium emission in the K(D_1) 769.9 nm line in co-added HIRES spectra and measured an intensity of 1.0 R. This intensity, in combination with a simultaneously measured Na(D_1) line intensity of 20 R, the commonality of the presumed production mechanisms of Na^* and K^*, their known kinetics, and an assumed [Na]/[K] ratio, sets the efficiency of the Na^* production to an upper limit of 0.1 and suggests that the K^* production mechanism is an order of magnitude more efficient. The same spectra also suggest an upper limit for the likely time-averaged intensity of the Li(D_1,D_2) lines at 670.8 nm of 0.015 mR. Slanger et al. [2000] HIRES spectra to measure several Balmer-series hydrogen lines in the geocorona, whose positions and intensities are consistent with primarily solar hydrogen Lyman line fluorescence excitation, either directly or via subsequent radiative cascade following high level excitation by other Lyman lines.

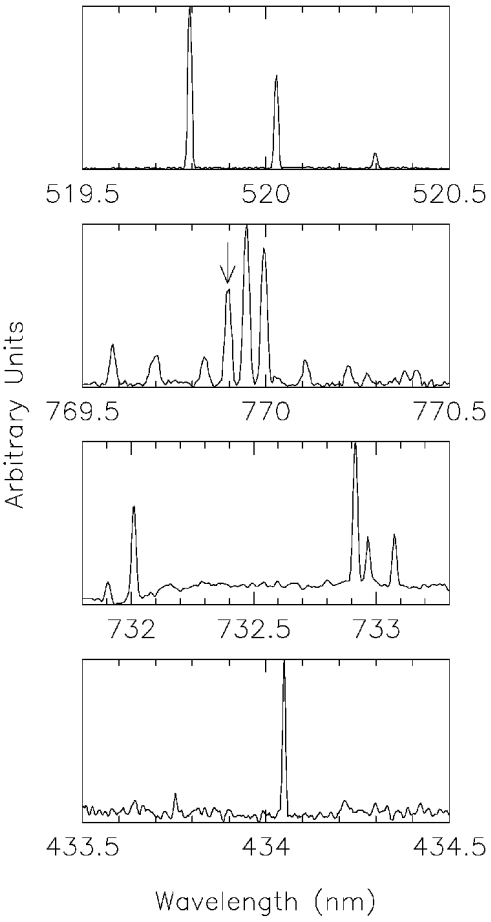

Figure 10. Segments from Keck/HIRES and VLT/UVES sky spectra showing various weak nightglow emission features. The top panel shows the N(^{2}D-^{4}S) doublet lines at 519.8 and 520.0 nm and the 9-2 Q_1(1.5) OH Meinel line at 520.3 nm; the arrow in the second panel shows the K(D_1) line at 769.9 nm adjacent to several 4-0 OH Meinel band and O_2($b^1\Sigma^+_g$ - $X^3\Sigma^-_g$) 1-1 band lines; the third panel shows the two O^+(^{2}P-^{2}D) doublets at 732.0 and 733.0 nm adjacent to the 8-3 P_2 (2.5) OH Meinel band line at 732.9 nm; the bottom panel shows the H_γ geocoronal line.

The intensity ratio of the N(^{2}D-^{4}S) doublet components at 519.8 and 520.0 nm has been measured from several flux-calibrated Keck/ESI spectra.[*Sharpee et al*., in preparation] The ratio of 519.8/520.0 nm intensities is found to be stable throughout each night at around 1.76. This value confirms an *ab-initio* value of 1.79 recently calculated for the ratio by Froese Fischer and Taichev [2004] under the assumption that rapid collisions between N_2 and the fine structure

levels of the ^{2}D term enforce statistical equilibrium of their populations,[*Huestis*, 2004] but differs considerably from the NIST value for the ratio of 2.61 for the same conditions.

CONCLUSIONS

The given examples demonstrate the power of large echelle spectrographs in investigating and discovering new nightglow phenomena. Much of what has been described represent new areas of aeronomic investigation. Although there are a number of sources of good sky spectra, it would obviously be advantageous for the aeronomic community to have such instruments under our control. We are currently not able to study temporal behavior, because of the long integration times of the astronomers, and we can expect only limited data from mid- and high-latitudes. It would also be synergistic to have similar spectrographs clustered with other aeronomic instruments. Other desirable characteristics include the ability to obtain accurate intensity calibration over large wavelength ranges, in addition to very precise wavelength calibration of nightglow features.

REFERENCES

Allan, M., Measurement of Absolute Differential Cross Sections for Vibrational Excitation of O_2 by Electron Impact, *J. Phys. B, 28*, 5163-5175, 1995.

Bates, D. R., The Oxygen Nightglow, in *Progress in Atmospheric Physics*, edited by R. Rodrigo, J. J. López-Moreno, M. López-Puertas, and A. Molina, pp. 3-31, Kluwer Academic, 1988.

Bloemink, H. I., R. A. Copeland, and T. G. Slanger, Collisional Removal of Vibrationally-Excited $O_2(b^1\Sigma_g^+, \upsilon = 1, 2)$ by O_2, N_2, and CO_2, *J. Chem. Phys.*, *109*, 4237-4245, 1998.

Chamberlain, J. W., The Blue Airglow Spectrum, *Ap. J.*, *128*, 713-717, 1958.

Chamberlain, J. W., The Ultraviolet Airglow Spectrum, *Ap. J. 123*, 277-286, 1955.

Charters, P.E., R. G. Macdonald, and J. C. Polanyi, Formation of Vibrationally Excited OH by the Reaction H + O_3, *Appl. Optics, 10*, 1747-1754, 1971.

Cierpka, K., M. J. Kosch, H. Holma, A. J. Kavanagh, and T. Hagfors, Novel Fabry-Perot Interferometer Measurements of F-region ion Temperatures, *Geophys. Res. Lett., 30,* 10.1029/2002GL015833, 2003

Colina, L. and R. C. Bohlin, Absolute Flux Calibration of Optical Spectrophotometric Standard Stars, *Astron. J.* 108, 1931-1935, 1994.

Cosby, P. C., T. G. Slanger, and D. E. Osterbrock, High Rotational Levels of OH Observed in Nightglow Meinel Band Emission, *Eos Trans. AGU, 80(17)*, Spring Meet. Suppl., S252, 1999

Escalante, V., and G. A. Victor, Effective Radiative Recombination Coefficients of Atomic Oxygen, *Planet. Space Sci.*, *40*, 1705-1718, 1992.

French, W.J.R., G. B. Burns, K. Finlayson, P. A. Greet, R. P. Lowe, and P. F. Williams, Hydroxyl (6-2) Airglow Emission Intensity Ratios for Rotational Temperature Determination, *Ann. Geophys*. *18*, 1293, 2000.

Froese Fischer, C. and G. Tachiev, Breit-Pauli Energy Levels, Lifetimes, and Transition Probabilities for Beryllium-like to Neon-like Sequences, *At. Data. Nucl. Data Tables, 87,* 1-184, 2004

Hanuschik, R. W., A Flux-Calibrated High-Resolution Atlas of Optical Sky Emission from UVES, *Astron. Astrophys., 407*, 1157-1164, 2003.

Huestis, D. L., Radiation, Collisional Mixing, Quenching, and Chemical Reactions of $N(2p^3\ ^2D_J)$, *J. Phys. Chem*., in press, 2004.

Hwang, E. S., A. Bergman, R. A. Copeland, and T. G. Slanger, Temperature Dependence of the Collisional Removal of $O_2(b^1\Sigma_g^+,\ \upsilon = 1$ and 2) at 110 - 260 K, and Atmospheric Applications, *J. Chem. Phys.*, *110*, 18-24, 1999.

Hwang, E. S., R. A. Copeland, R. M. Robertson, and T. G. Slanger, Collisional Removal of $O_2(a^1\Delta_g)$ v = 1,2 and Detection of $O_2(a^1\Delta_g)$ and $O_2(b^1\Sigma_g^+)$ from Photodissociation of Ozone at 310-340 nm, *Eos Trans. AGU*, *79*, F85, 1998.

Ingham, M. F., The Nightglow Spectrum, *Mon. Not. Royal Astron. Soc.*, *124*, 505-522, 1962.

Kalogerakis, K. S., A. Totth, P. C. Cosby, T. G. Slanger, and R. A. Copeland, Laboratory Studies of the Production of Highly Vibrationally Excited $O_2(a^1\Delta_g, b^1\Sigma_g^+)$ from $O_2(A^3\Sigma_u^+)$ Relaxation, *EOS Trans*. *AGU, 81*, F944, 1998.

Kalogerakis, K. S., D. L. Huestis, P. C. Cosby, T. G. Slanger, and R. A. Copeland, High Vibrational Levels of $O_2(b)$ and $O_2(a)$, in *56th International Symposium on Molecular Spectroscopy*, Columbus, OH, 2001.

Kalogerakis, K. S., R. A. Copeland, and T. G. Slanger, Collisional Removal of $O_2(b^1\Sigma_g^+$, v = 2,3), *J. Chem. Phys.*, *116,* 4877-4885, 2002.

Kirchhoff, V.W.J.H., and H. Takahashi, First Sodium Nightglow Results from Natal, *Planet. Space Sci.*, *33* (6), 757-760, 1985.

Klenerman, D., and I.W.M. Smith, Infrared Chemiluminescence Studies Using a SISAM Spectrometer: Reactions Producing Vibrationally Excited OH, *J. Chem. Soc. Faraday Trans.* 2, 83, 229-241, 1987.

Krasnopolsky, V. A., Oxygen Emissions in the Night Airglow of the Earth, Venus and Mars, *Planet. Space Sci.*, *34*, 511-518, 1986.

Krassovsky, V. I., N. N. Shefov, and V. I. Yarin, Atlas of the Airglow Spectrum (3000-12400 Å), *Planet. Space Sci*. *9*, 883-915, 1962.

Lancaster, R. S., L. S. Waldrop, R. B. Kerr, J. Noto, S. C. Solomon, C. A. Tepley, R. Garcia, and J. Friedman, Brightness Measurements of the Nighttime OI 8446 A Airglow Emission from the Millstone Hill and Arecibo Observatories, *J. Geophys. Res.*, *105*, 5275-90, 2000.

Lancaster, R. S., R. B. Kerr, K. Ng, J. Noto, and M. Franco, Recent Observations of the OI 8446 Å Emission over Millstone Hill, *Geophys. Res. Lett.*, *21* (9), 829-832, 1994.

Lee, L. C., and T. G. Slanger, Observations of O(^1D - ^3P) and $O_2(b^1\Sigma_g^+ - X^3\Sigma_g^-)$ following O_2 photodissociation, *J. Chem. Phys.*, *69*, 4053-4060, 1978.

McDade, I. C., E. J. Llewellyn, R.G.H. Greer, and D. P. Murtagh, ETON 3: Altitude profiles of the nightglow continuum at green and near infrared wavelengths`, *Planet. Space Sci.*, *34*, 801-810, 1986.

Meier, R. R., Ultraviolet Spectroscopy and Remote Sensing of the Upper Atmosphere, *Space Sci. Rev.*, *58*, 1-185, 1991.

Meriwether, J. W., A Review of the Photochemistry of Selected Nightglow Emissions from the Mesopause, *J. Geophys. Res*. *94*, 14629-14646, 1989.

Minaev, B. F., and L. B. Yashchuk, Electronic-Rotational Coupling and c-b Transition Probability in the Oxygen Molecule, *High Energy Chemistry*, *38* (4), 209-214, 2004.

Moore, C. E., Atomic Energy Levels and their Derived Standards (National Bureau of Standards Circular 467; Washington: U.S. Dept. of Commerce), 47, 1949

Oke, J. B., Faint Spectrophotometric Standard Stars, *Astron. J., 99*, 1621-1631, 1990

Osterbrock, D. E., J. P. Fulbright, A. R. Martel, M. J. Keane, S. C. Trager, and G. Basri, Night-Sky High-Resolution Spectral Atlas of OH and O_2 Emission Lines for Echelle Spectrograph Wavelength Calibration, *Pub. Astron. Soc. Pacific*, *108*, 277-308, 1996.

Rees, M. H., G. J. Romick, and A. E. Belon, The Intensity of the Sodium D lines in the Auroral Zone, *Ann. Geophys.*, *31* (2), 311-320, 1975.

Sharpee, B. D., T. G. Slanger, D. L. Huestis, and P. C. Cosby, Measurements of the Singly Ionized Oxygen Auroral Doublet Lines λλ7320, 7330 using High-Resolution Sky Spectra, *Ap. J., 606*, 605-610, 2004

Sipler, D. P., and M. A. Biondi, Interferometric Studies of the Twilight and Nightglow Sodium D-Line Profiles, *Planet. Space Sci.*, *26*, 65-73, 1978.

Sivjee, G. G., Airglow Hydroxyl Emissions, *Planet. Space Sci*. *40*, 235-242 (1992).

Slanger, T. G. and D. E. Osterbrock, Aeronomy-Astronomy Collaboration Focuses on Nighttime Terrestrial Atmosphere, *EOS Trans*. *AGU*, 79, 152-154, 1998.

Slanger, T. G. and D. E. Osterbrock, Investigations of Potassium, Lithium, and Sodium Emission in the Nightglow and OH Calibration, *J. Geophys. Res, 105(D1),* 1425-1429, 2000Adler-Golden, S., Kinetic Parameters for OH Nightglow Modeling Consistent with Recent Laboratory Measurements, *J. Geophys. Res*. *102*, 19969-19976, (1997.

Slanger, T. G., D. L. Huestis, P. C. Cosby, and D. E. Osterbrock, Accurate Atomic Line Wavelengths from Astronomical Sky Spectra, *J. Chem. Phys., 113*, 8514-8520, 2000

Slanger, T. G., D. L. Huestis, P. C. Cosby, and R. R. Meier., Oxygen Atom Rydberg Emission in the Equatorial Ionosphere from Radiative Recombination, *J. Geophys. Res*. in press, 2004b.

Slanger, T. G., P. C. Cosby, and D. L. Huestis, A New O_2 Band System: The $c^1\Sigma_u^-$ - $b^1\Sigma_g^+$ Transition in the Terrestrial Nightglow, *J. Geophys. Res*. *108* (A2), 1089, 2003b.

Slanger, T. G., P. C. Cosby, and D. L. Huestis, Ground-Based Observation of High-Altitude High-Temperature Emission in the O_2 Atmospheric Band Nightglow, *J. Geophys. Res.*, *108* (A7), 10.1029/2003JA009885, 2003a.

Slanger, T. G., P. C. Cosby, D. L. Huestis, and A. M. Widhalm, Nightglow Vibrational Distributions in the *A* and *A′* states of O_2 Derived from Astronomical Sky Spectra, *Ann. Geophys.*, in press, 2004a.

Slanger, T. G., P. C. Cosby, D. L. Huestis, and D. E. Osterbrock, Vibrational Level Distribution of $O_2(b^1\Sigma_g^+, \upsilon = 0\text{-}15)$ in the Mesosphere and Lower Thermosphere Region, *J. Geophys. Res.*, *105*, 20557-20564, 2000.

Tinsley, B. A., A. B. Christensen, J. Bittencourt, H. Gouveia, P. D. Angreji, and H. Takahashi, Excitation of Oxygen Permitted Line Emission in the Tropical Nightglow, *J. Geophys. Res.*, *78*, 1174-1186, 1973.

Wilkinson, P. G., and R. S. Mulliken, Forbidden Band Systems in Nitrogen. II. The *a′-X* System in Absorption, *J. Chem. Phys.*, *31*, 674-679, 1959.